ACCEPTED MANUSCRIPT
The Journal of Chemical Physics
AIP Publishing
This is the author's peer reviewed, accepted manuscript. However, the online version of record will be different from this version once it has been copyedited and typeset.
PLEASE CITE THIS ARTICLE AS DOI: 10.1063/5.0328356

The X-ray absorption spectrum of the propargyl radical, $C_3H_3^{\bullet}$

Dorothee Schaffner,[1] Theo Juncker von Buchwald,[2] Jacob Pedersen,[2,3] Andreas Rasp,[1] Emil Karaev,[1] Valentin von Laffert,[1] Alessio Bruno,[4] Michele Alagia,[5] Stefano Stranges,[4,5] Ingo Fischer,[1,a)] and Sonia Coriani[2,b)]

[1)] *Institute of Physical and Theoretical Chemistry, University of Würzburg, D-97074 Würzburg, Germany.*

[2)] *DTU Chemistry, Technical University of Denmark, DK-2800 Kgs. Lyngby, Denmark.*

[3)] *Department of Chemistry, Norwegian University of Science and Technology, N-7491 Trondheim, Norway.*

[4)] *Dipartimento di Chimica e Tecnologia dei Farmaci, Università degli Studi di Roma "La Sapienza", piazzale Aldo Moro 5, I-00185 Rome, Italy.*

[5)] *CNR - Istituto Officina dei Materiali (IOM), Laboratorio TASC, I-34149 Trieste, Italy.*

(Dated: 15 May 2026)

ACCEPTED MANUSCRIPT

The Journal of Chemical Physics

AIP Publishing

This is the author's peer reviewed, accepted manuscript. However, the online version of record will be different from this version once it has been copyedited and typeset.
PLEASE CITE THIS ARTICLE AS DOI: 10.1063/5.0328356

We report a combined experimental and computational study of the near-edge X-ray absorption fine structure (NEXAFS) spectrum of the propargyl radical, $C_3H_3^{\bullet}$. As a central intermediate in the formation of polycyclic aromatic hydrocarbons, the propargyl radical is a species of considerable relevance in combustion and astrochemistry and was here generated by pyrolysis from propargyl bromide. The NEXAFS spectrum shows a pronounced band at 282.2 eV corresponding to transitions from carbon 1s orbitals to singly occupied molecular orbitals. *Ab initio* calculations reveal that two transitions to the lowest-lying states 1 $^2A_1$ and 2 $^2A_1$, which take place from the C1s orbital of the two terminal carbon atoms, contribute to this band. In addition, a 420 meV spacing of the first band is visible and is assigned to a vibrational progression in the symmetric CH_2 stretch. Transitions at higher energies are also described reasonably well by theory. The fragmentation pattern was investigated at the different resonant transitions and shows the cleavage of one as well as both C–C bonds.

Keywords: propargyl, NEXAFS, X-ray spectroscopy, computation, carbon edge

[a)] E-mail: ingo.fischer@uni-wuerzburg.de (experiment)

[b)] E-mail: soco@kemi.dtu.dk (theory)

ACCEPTED MANUSCRIPT
The Journal of Chemical Physics
AIP Publishing
This is the author's peer reviewed, accepted manuscript. However, the online version of record will be different from this version once it has been copyedited and typeset.
PLEASE CITE THIS ARTICLE AS DOI: 10.1063/5.0328356

I. INTRODUCTION

The mechanism of the formation of polycyclic aromatic hydrocarbons (PAHs) is a major research topic in astrochemistry as well as in combustion science.[1–4] In interstellar space, PAHs and their cations are investigated as possible carriers of the diffuse interstellar bands (DIB) as well as the unidentified infrared bands (UIB).[5] They have been postulated to comprise a significant part of the carbon budget in space.[6] However, the formation mechanism of PAHs in the low pressure and low temperature environment of space is an open question.[3] Barrierless or low-barrier reactions, such as ion-molecule and radical-radical reactions, offer a possible explanation. In combustion, the dimerization of propargyl, $C_3H_3^{\bullet}$, was found to be an efficient reaction that proceeds in a sequence of barrierless steps to benzene and phenyl radical.[7,8] Propargyl, shown on the right-hand side of Scheme 1, is a resonantly stabilized radical of C_{2v} symmetry with a $\tilde{X}\ ^2B_1$ ground state.[9] For the nominal resonance structures ethynyl methyl ($H_2C^{\bullet}-C{\equiv}CH$) and allenyl ($H_2C{=}C{=}C^{\bullet}H$), a ratio of 61% to 39% was inferred from recent microwave measurements analyzing the spatial distribution of the unpaired electron.[10] Propargyl is a well-known intermediate in flames and plasmas and has recently been detected in the cold dark Taurus Molecular Cloud (TMC-1)[11,12] where the corresponding cationic species has been observed as well.[13] The detection was based on prior laboratory microwave spectra.[14] It was suggested that propargyl is "one of the most abundant radicals detected in TMC-1, and it is probably the most abundant organic radical with a certain chemical complexity ever found in a cold dark cloud."[11] Most likely, it is also involved in the atmospheric chemistry of the Saturn moon Titan.[15] Given its abundance, the propargyl radical may be involved in the synthesis of aromatic molecules in space as well. For example, the ion-molecule reaction $H_2CCCH^{\bullet} + C_3H_3^+ \rightarrow C_6H_5^+ + H^{\bullet}$ has been suggested to be an efficient source for formation of the phenyl cation.[16] Due to the importance of the propargyl radical in astrochemistry and in combustion chemistry, its spectroscopy and chemistry have been broadly investigated. Specifically, infrared,[17,18] UV/Vis[19,20] and photoelectron spectra,[21–23] including a study that followed the steps to benzene formation,[24] have been reported. The photodissociation has been studied by H-atom photofragment spectroscopy,[25] high-n Rydberg atom time-of-flight (HRTOF) spectroscopy,[26] and in a Laval nozzle expansion.[27] Hydrogenation reactions of $C_3H_3^+$ and related cations important for carbon chemistry in space have been studied in ion traps.[28,29] The bimolec-

ACCEPTED MANUSCRIPT
The Journal of Chemical Physics
AIP Publishing
This is the author's peer reviewed, accepted manuscript. However, the online version of record will be different from this version once it has been copyedited and typeset.
PLEASE CITE THIS ARTICLE AS DOI: 10.1063/5.0328356

ular recombination of propargyl was studied in the gas-phase and branching ratios of the isomeric C_6H_6 reaction products were determined.[30,31] The further efficient growth of PAHs by a subsequent addition of propargyl units to the first ring has been investigated by IR/UV ion dip spectroscopy.[32] Both the structure as well as reactions of the propargyl radical have also been investigated computationally, with a focus on the propargyl dimerization.[9,33] Possible mechanisms for PAH formation and growth reactions that include propargyl as one reactant have been studied experimentally[34–37] and computationally.[38–40] Propargyl has also been investigated as precursor for the formation of nitrogen-containing PAHs (PANHs) in space.[41]

In contrast to the investigations in other spectral regions, the response of polyatomic organic radicals to X-ray excitation has hardly been studied. The astrochemical relevance of this topic originates from the X-ray emission in young stellar objects that might have a significant influence on the circumstellar molecular composition.[42] So far, X-ray absorption near the first C1s ionization threshold (XAS, NEXAFS) in hydrocarbon radicals has only been investigated for allyl, $C_3H_5^{\bullet}$,[43] methyl, $CH_3^{\bullet}$,[44] and its isotopomer $CD_3^{\bullet}$,[45] as well as *tert*-butyl, $C_4H_9^{\bullet}$.[46] A recent study focused on the C1s NEXAFS spectroscopy of different isomeric $C_3H_3^+$ cations, including the propargylium ion. There, site-specific resonances and fragmentation channels leading to doubly charged fragments were investigated.[47]

In the present work, we address the NEXAFS spectroscopy of neutral propargyl, one of the astrochemically most important radicals, in a combined experimental and computational study. This work will also help to identify the propargyl radical in future studies using time-resolved X-ray spectroscopy.

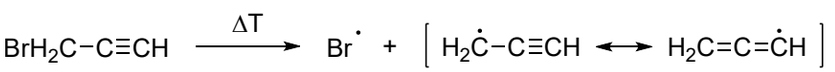
II. METHODS

A. Experimental

The experiments were carried out at the Gas Phase Photoemission beamline at the Elettra Synchrotron, Trieste/IT. The setup has been detailed previously,[48,49] but a brief description is given in the following. Synchrotron light at the C1s edge and at 21.2 eV was provided by an undulator and spectrally dispersed by a variable angle, spherical grating type monochromator. Different gratings were used for different photon energy regions, and the photon

ACCEPTED MANUSCRIPT
The Journal of Chemical Physics
AIP Publishing
This is the author's peer reviewed, accepted manuscript. However, the online version of record will be different from this version once it has been copyedited and typeset.
PLEASE CITE THIS ARTICLE AS DOI: 10.1063/5.0328356

energy resolution was controlled by the entrance and exit slit width.



Scheme 1. Generation of the propargyl radical, $H_2CCCH^{\bullet}$, by pyrolysis of propargyl bromide. On the right-hand side the ethynyl methyl and allenyl resonance structures of the propargyl radical are shown.

The precursor propargyl bromide (stabilized with MgO) was purchased from TCI and used after several freeze-pump-thaw cycles. Propargyl bromide was cooled to −30 °C, and the vapor of the precursor diluted in helium (dilution of 0.1 %) passed through a resistively heated SiC pyrolysis tube. Scheme 1 shows the pyrolysis of propargyl bromide that yields the propargyl radical and a bromine atom.[21,25] The pyrolysis products were expanded into the vacuum and entered the experimental chamber through a skimmer. The molecular beam was crossed by the synchrotron radiation, and the resulting electrons and ions were extracted in opposite directions. Electrons and ions were detected in coincidence by a single start-multiple stop technique. The electrons were detected by an MCP detector, set close to the ionization region, and used as start signal for the ion time-of-flight (TOF). Ions were detected by a Wiley-McLaren TOF mass spectrometer.

The pyrolytic conversion of the precursor according to Scheme 1 was investigated by valence photoionization mass spectrometry at 21.2 eV. For C1s NEXAFS spectra the total electron yield (TEY) was recorded while the photon energy was scanned. The photon flux was monitored by a photodiode and used for normalization of the spectra. To correct for the helium background in the spectra, a spectrum of pure helium was measured and subtracted. In a diagnostic chamber in front of the experimental chamber, methane was measured simultaneously to calibrate the photon energy by its C1s → 3p-Rydberg transition at 288.00 eV.[50] The photon bandwidth around the C1s edge was 50 meV. The C1s NEXAFS spectra in the region 280.3–297.2 eV were measured with a step size of 20 meV and an acquisition time of 45 s (pyrolysis at 35 W heating power) and 35 s (pyrolysis off) per data point. High-resolution spectra in the range 281.3–283.3 eV were measured with a step size of 10 meV and an acquisition time of 75 s. Valence photoionization mass spectra at 21.2 eV were recorded with acquisition times between 300 s and 1800 s, while mass spectra at the C1s edge were acquired for 6000 s.

ACCEPTED MANUSCRIPT
The Journal of Chemical Physics
AIP Publishing
This is the author's peer reviewed, accepted manuscript. However, the online version of record will be different from this version once it has been copyedited and typeset.
PLEASE CITE THIS ARTICLE AS DOI: 10.1063/5.0328356

B. Computational

Two *ab initio* electronic structure approaches were primarily adopted for the computational study of the electronic transitions, namely the frozen-core core-valence-separated equation-of-motion coupled cluster singles and doubles (fc-CVS-EOM-CCSD) method,[51] and the extended core-valence-separated second-order algebraic diagrammatic construction (CVS-ADC(2)-x) method,[52] as implemented in `Q-Chem`.[53] A preliminary basis set study was performed at the fc-CVS-EOM-CCSD level using both restricted-open (ROHF) and unrestricted (UHF) Hartree-Fock reference orbitals, and the 6-311++G**,[54–56] cc-pVTZ,[57] and aug-cc-pVTZ[58] basis sets on all atoms. Unrestricted Hartree-Fock reference orbitals and the aug-cc-pVTZ basis set were used at the CVS-ADC(2)-x level. Core ionization energies were obtained at the fc-CVS-EOM-IP-CCSD level. The core-valence-separated coupled cluster linear response (LR) approach[59] at CCSD and coupled cluster singles, doubles, and triples (CCSDT) levels of theory, as implemented in the `MRCC`[60] code, was additionally used to investigate how improvement of the electronic structure method by inclusion of triple excitations impacted the spectra of the first four bright electronic transitions. The cc-pVDZ basis set was used for this analysis.

We used the CCSD(T*)-F12a[61,62]/cc-pVTZ-F12[63]-optimized molecular geometry (planar C_{2v} structure) from Botschwina and Oswald[9] in all calculations of the purely electronic spectra. This structure is rather similar to the recently reported semi-experimental equilibrium geometry of Changala *et al.*[10] The bond lengths of both structures are reported in Table S9 in the SI. As observed by the authors of Ref. 10, the deviation of the C–C bond lengths in the ground state of propargyl from pure single, double and triple bonds are "[...] evidence of π-delocalization of the unpaired electron along the carbon backbone".[10]

Natural transition orbitals (NTOs)[51,64] were computed at the corresponding fc-CVS-EOM-CCSD and CVS-ADC(2)-x levels of theory and used for the assignment of the spectral peaks. The spectra were constructed from the computed excitation energies and oscillator strengths using a Lorentzian convolution with a full width at half maximum (FWHM) broadening of 200 meV. All calculations were carried out on DTU HPC resources.[65]

Three different strategies were adopted to investigate vibrational effects in the spectrum. In the first strategy, the nuclear ensemble approach (NEA),[66] we sampled 200 vibrational structures of the ground state using a Wigner sampling at a temperature of 300 K. The

ACCEPTED MANUSCRIPT
The Journal of Chemical Physics
AIP Publishing
This is the author's peer reviewed, accepted manuscript. However, the online version of record will be different from this version once it has been copyedited and typeset.
PLEASE CITE THIS ARTICLE AS DOI: 10.1063/5.0328356

ground state frequencies used for sampling the vibrational structures are calculated from a B3LYP[67]/aug-cc-pVTZ optimized geometry. For all structures the NEXAFS spectrum was then calculated using both fc-CVS-EOM-CCSD and CVS-ADC(2)-x with the aug-cc-pVTZ basis set.

In the second and third strategy, both a time-independent (TI) and a time-dependent (TD) quantum approach were utilized for the calculation of the vibrational structure of the selected electronic transitions in the NEXAFS spectrum.[68,69] The (eigenstate-free) TD approach delivers directly the vibrationally resolved spectral profile, whereas the TI approach is based on the individual stick transitions of all possible vibronic states, which are then broadened. The potential energy surfaces (PES) associated with the electronic states involved in the transition that are required by both methods were obtained from the harmonic Vertical Gradient (VG)[68,70,71] and Adiabatic Shift (AS)[68,71] approximations, respectively. `FCclasses3`[69] was used for these calculations. The VG and AS approximations both utilize the ground state energy, gradient, and Hessian as well as the excitation energy and a 1-norm dipole moment along the same direction (x, y, and z) as the transition dipole moment. The two methods differ in the way they treat the excited state geometry and gradient when reconstructing the PES of the final electronic state.[68] For the VG approximation (also known as linear coupling model[70]), the ground state geometry is used also for the excited state, and the excited state gradient is calculated at this geometry. In the AS approximation, the excited state geometry is optimized, and the excited state gradient is practically zero within the chosen optimization threshold. The ground and excited state(s) share the same normal modes and frequencies, as the same Hessian is used for both.[68] The spectra are scaled afterwards using the transition dipole strength. For the ground state we used a UMP2/aug-cc-pVDZ optimized geometry obtained using Gaussian.[72] Excited state geometry optimizations at the ADC(2)-x/aug-cc-pVDZ level of the first three bright states were carried out using `PySCF`[73,74] for the Hartree-Fock calculation, `ADCC`[75] for the ADC(2)-x excitation energy calculation, `cvs-adc-grad`[76] for the excited state gradient, and `geomeTRIC`[77] for the numerical geometry optimization. The vibrationally resolved spectral bands were broadened by a Voigt function with a Gaussian FWHM of 50 meV and a Lorentzian FWHM of 100 meV, corresponding to the experimental photon bandwidth and the approximate lifetime width of the C1s core hole, respectively. We computed both TI and TD spectra at 0 K, as well as TD ones at 300 K. We refer to Section S2.1 in the Supplementary Information

AIP Publishing
The Journal of Chemical Physics
ACCEPTED MANUSCRIPT
This is the author's peer reviewed, accepted manuscript. However, the online version of record will be different from this version once it has been copyedited and typeset.
PLEASE CITE THIS ARTICLE AS DOI: 10.1063/5.0328356

Propargyl radical

(SI) for additional computational details.

ACCEPTED MANUSCRIPT
The Journal of Chemical Physics
AIP Publishing
This is the author's peer reviewed, accepted manuscript. However, the online version of record will be different from this version once it has been copyedited and typeset.
PLEASE CITE THIS ARTICLE AS DOI: 10.1063/5.0328356

III. RESULTS AND DISCUSSION

A. Experimental NEXAFS spectrum

Figure 1 shows the comparison of the valence photoionization mass spectrum without pyrolysis (upper trace, a) and with optimized pyrolysis conditions (lower trace, b). The spectra were recorded at 21.2 eV to confirm the pyrolytic conversion of the precursor according to Scheme 1. Both spectra were normalized to the mass signal of the carrier gas helium at m/z 4. Without pyrolysis the parent ion of the precursor, $C_3H_3Br^+$, is observed at m/z 118 and 120 with a double peak structure originating from the two isotopes ^{79}Br and ^{81}Br. Dominant signals at m/z 39, 38, and a weaker one at m/z 37 result from the dissociative photoionization (DPI) of the precursor to $C_3H_3^+$, $C_3H_2^+$ and C_3H^+. For $C_3H_3^+$ an appearance energy of 10.88 eV was determined previously,[78] and also C_3H^+ was formerly identified as a DPI product of the precursor in spectra taken at 15.77 eV.[79] Measurements with pyrolysis were performed at a power of 35 W, corresponding to a SiC capillary temperature of approximately 1200 °C. The radical, which has a rich vibrational manifold of states with many low frequency vibrational modes, is assumed to be in the interaction region vibrationally cold, due to the efficient adiabatic expansion in the jet source. The corresponding mass spectrum in Figure 1b) shows new bromine signals from the pyrolysis and only a negligibly small $C_3H_3Br^+$ mass signal of the unpyrolysed precursor. The peak at m/z 39, which is lower in intensity and narrower than in the spectrum of the pure precursor, is likely to originate from both the pyrolytically generated propargyl radical $C_3H_3^\bullet$ and the DPI product of the unconverted precursor. The latter shows a broad pedestal below this peak, which results from the kinetic energy release in the DPI. Compared to the pure precursor spectrum the relative intensity of both $C_3H_2^+$ and C_3H^+ to $C_3H_3^+$ is increased. $C_3H_2^+$ and C_3H^+ are known DPI products of the propargyl radical that are associated with appearance energies of 12.5–13 eV and >15.5 eV.[79]

NEXAFS spectra at the C1s edge were recorded as TEY with and without pyrolysis and are shown in the upper trace of Figure 2. The spectrum of the precursor (black line) sets in above 284 eV and shows an intense signal around 286 eV with a double peak structure characterized by a spacing of 300 meV. At higher photon energies several less intense signals are observed, and the TEY increases above 291 eV, when the C1s ionization thresholds are

ACCEPTED MANUSCRIPT
The Journal of Chemical Physics
AIP Publishing
This is the author's peer reviewed, accepted manuscript. However, the online version of record will be different from this version once it has been copyedited and typeset.
PLEASE CITE THIS ARTICLE AS DOI: 10.1063/5.0328356

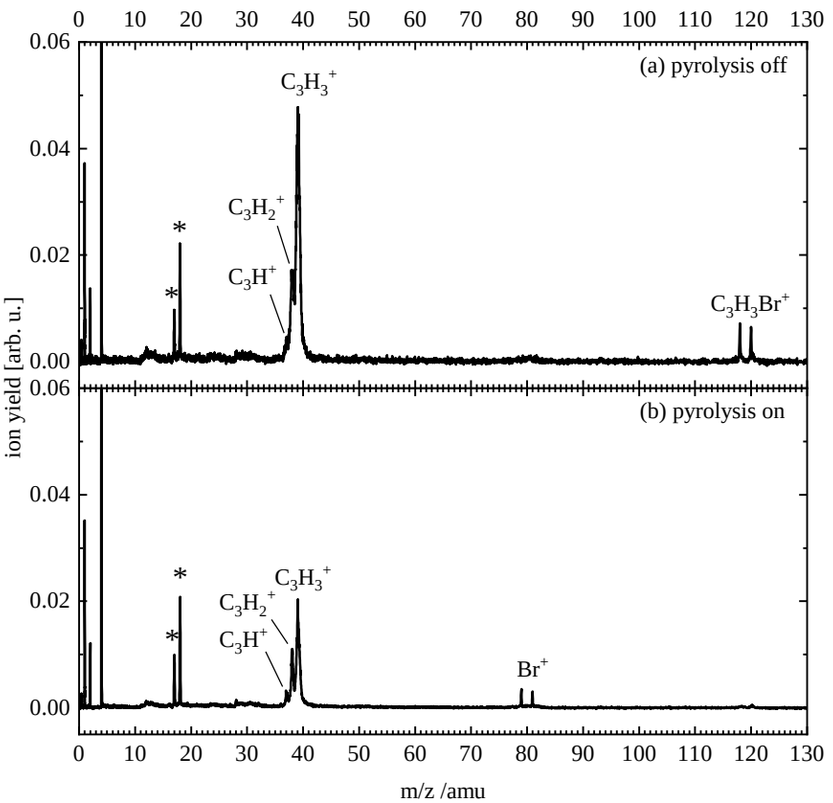


FIG. 1. TOF mass spectra at 21.2 eV with (a) pyrolysis off and (b) pyrolysis on. The spectra were normalized to the He^+ signal at m/z 4. Asterisks indicate water as impurity.

approached. The absorption spectrum with pyrolysis (red line) corresponds to the spectrum of the precursor and the propargyl radical. A new band is found at 282.2 eV and its shift to much lower photon energies compared to the pure precursor is a fingerprint of an open shell species. It is attributed to a transition from a C1s orbital into a singly occupied molecular orbital (SOMO) of the unpaired electron of the propargyl radical (Section III B). The spectrum of the pure radical was obtained by subtraction of the spectra with and without pyrolysis, whereby the onset and the maximum of the band at 286 eV were used to scale the spectrum of the pure precursor. The resulting spectrum of the propargyl radical is shown in Figure 2(b). Band A corresponds to the transition into the SOMO and shows a vibrational progression of 420 meV. A broad structureless feature is found at 284.8 eV (B), which is red-shifted with respect to the main signal of the precursor. In contrast, new signals at 286.0 eV (C), 286.6 eV (D) and 288.2 eV (E) are located at the maximum or the high energy flank of the precursor's main signal and are visible from Figure 2(a).

ACCEPTED MANUSCRIPT
The Journal of Chemical Physics
AIP Publishing
This is the author's peer reviewed, accepted manuscript. However, the online version of record will be different from this version once it has been copyedited and typeset.
PLEASE CITE THIS ARTICLE AS DOI: 10.1063/5.0328356

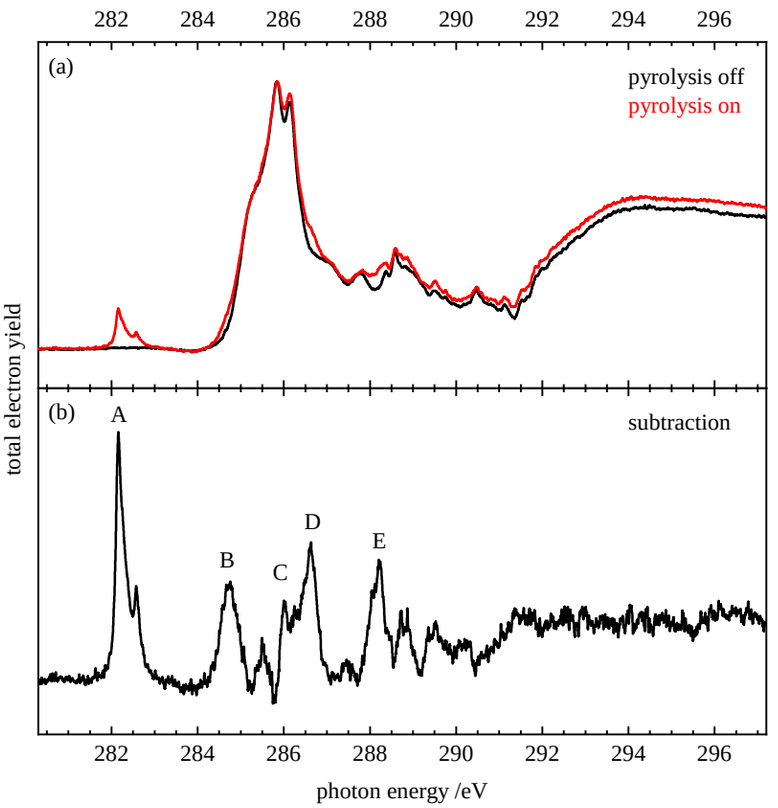


FIG. 2. (a) C1s NEXAFS spectra of the precursor propargyl bromide without and with pyrolysis. (b) C1s NEXAFS spectrum of the propargyl radical obtained from subtraction.

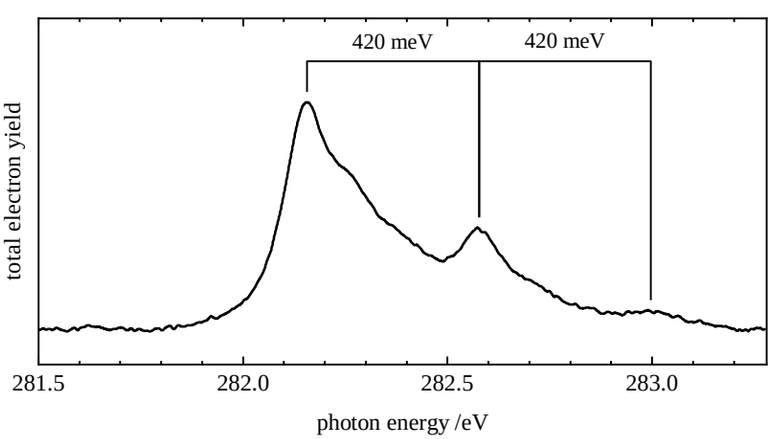


FIG. 3. High resolution NEXAFS spectrum of the C1s to SOMO transition (band A).

To investigate the vibrational structure of the lowest band in the propargyl spectrum, band A was scanned with a smaller step size and is displayed in Figure 3. A progression with three components was identified. The spacing of 420 meV suggests the excitation of a C–H stretching vibration upon the C1s to SOMO excitation. The first component at 282.16 eV

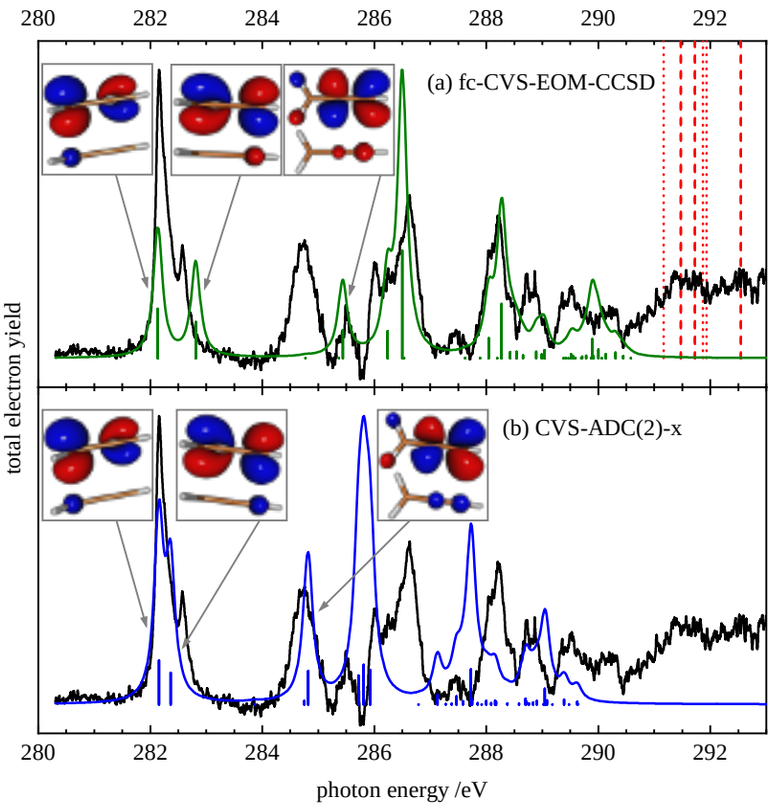


FIG. 4. Comparison between experimental NEXAFS spectrum (black line) and computed (a) fc-CVS-EOM-CCSD/aug-cc-pVTZ and (b) CVS-ADC(2)-x/aug-cc-pVTZ NEXAFS spectra of the propargyl radical using UHF reference orbitals. The sticks were convoluted with a Lorentzian lineshape function with a FWHM of 200 meV. The vertical red dashed lines are the fc-CVS-EOM-IP-CCSD ionization potentials to singlet ionic states and the dotted ones to triplet ionic states.

(and possibly also the second one at 282.58 eV) also reveals a high-energy shoulder that may belong to a simultaneously excited bending vibration. To understand how electronic and/or vibrational excitations influence the appearance of this first band (A), a theoretical assignment of the spectrum is indispensable.

B. Computational results and spectral assignment

For the computational discussion, we denote the CH_2 carbon of the propargyl radical as C1 and the CH as C3, with the carbon in between as C2. The bands in Figure 2(b) are assigned based on *ab initio* calculations at the fc-CVS-EOM-CCSD and CVS-ADC(2)-x levels of theory using the aug-cc-pVTZ basis set. All computed excitation energies and

ACCEPTED MANUSCRIPT
The Journal of Chemical Physics
AIP Publishing
This is the author's peer reviewed, accepted manuscript. However, the online version of record will be different from this version once it has been copyedited and typeset.
PLEASE CITE THIS ARTICLE AS DOI: 10.1063/5.0328356

ACCEPTED MANUSCRIPT
The Journal of Chemical Physics
AIP Publishing
This is the author's peer reviewed, accepted manuscript. However, the online version of record will be different from this version once it has been copyedited and typeset.
PLEASE CITE THIS ARTICLE AS DOI: 10.1063/5.0328356

their associated oscillator strengths are summarized in Table S2 of the SI. Additional fc-CVS-EOM-CCSD results obtained with other basis sets are collected in Table S3 and displayed in Figure S2. NTOs are given in Tables S4 and S5, for fc-CVS-EOM-CCSD and CVS-ADC(2)-x, respectively. A comparison of the simulated fc-CVS-EOM-CCSD spectra in Figure S2 shows that a change in basis set leads to a shift in the spectrum when compared to the experimental results and the splitting of the first two transitions narrows when changing from an open-shell restricted to an unrestricted Hartree-Fock reference. Overall, the fc-CVS-EOM-CCSD spectral profiles are rather similar.

Comparing the unrestricted fc-CVS-EOM-CCSD/aug-cc-pVTZ spectrum to the CVS-ADC(2)-x/aug-cc-pVTZ one in Figure 4, we note that the energy separation of the first two transitions narrows further at the CVS-ADC(2)-x level, and the third transition shifts in position and increases in intensity, overlapping with the experimental band B at 284.8 eV.

Based on the computed spectral data and NTOs, band A at 282.2 eV is assigned to a combination of the transitions to the 1 ^{2}A$_1$ state (C1 1s $\rightarrow$ SOMO) and to the 2 ^{2}A$_1$ state (C3 1s $\rightarrow$ SOMO). These are located at 282.15 eV and 282.36 eV, respectively, by CVS-ADC(2)-x, and at 282.14 eV and 282.81 eV by fc-CVS-EOM-CCSD. We note that the SOMO particle NTO is of (ethynyl methyl) p(C1)-π(C2-C3) character for the transition to the 1 ^{2}A$_1$ state, and of (allenyl) π(C1-C2)-p(C3) character for the transition to the 2 ^{2}A$_1$ state. This is suggestive of the core excitation taking place from either an ethynyl methyl or an allenyl resonance structure (compare Scheme 1).

The experimental band B at 284.8 eV overlaps with the CVS-ADC(2)-x transition to the 2 ^{2}A$_2$ state at 284.82 eV, which consists of a core excitation from the 1s orbitals of C2 and C3 to an in-plane π^* orbital (suggesting the presence of a triple bond between C2 and C3, as expected in the nominal ethynyl methyl resonance structure). The third transition in the fc-CVS-EOM-CCSD calculation is less intense and located at higher energy than the experimental band B (overlapping with the less intense peak at its right) but has the same character as the CVS-ADC(2)-x one.

Moving towards the region of bands C–D of the experimental spectrum (286.0–286.6 eV), we note that CVS-ADC(2)-x yields three dipole allowed transitions with sizable intensity, whereas fc-CVS-EOM-CCSD gives only two. In both cases, our computed transitions are slightly too closely spaced, yielding a narrower and more intense band when convoluted. Above 285.5 eV, the CVS-ADC(2)-x transitions are also more red-shifted than the fc-CVS-

ACCEPTED MANUSCRIPT
The Journal of Chemical Physics
AIP Publishing
This is the author's peer reviewed, accepted manuscript. However, the online version of record will be different from this version once it has been copyedited and typeset.
PLEASE CITE THIS ARTICLE AS DOI: 10.1063/5.0328356

EOM-CCSD ones, and do not overlap well with the experimental bands. Nonetheless, the C–D region of the experimental spectrum is dominated, according to our calculations with both methods, by transitions from the C2 1s orbital (with some mixing of the C3 one) to either the in-plane or the out-of-plane π^* particle NTOs (shown in Table S4 and S5).

As for the band E just above 288 eV in the experimental spectrum, several transitions, some with rather low intensity, contribute. At fc-CVS-EOM-CCSD level, two transitions are most intense, with the strongest one at 288.28 eV due to a C2 1s $\rightarrow$ (out-of-plane) π^*. Similarly, several transitions contribute to the band E at CVS-ADC(2)-x level, with the most intense one at 287.73 eV (again red-shifted compared to experiment), and the same character as the intense E transition from fc-CVS-EOM-CCSD.

We also computed core ionization energies for all three carbon atoms by the fc-CVS-EOM-IP-CCSD approach, summarized in Table S6 and given as red vertical lines in Figure 4 (UHF results). For the formation of a singlet cation, the lowest ionization energy of 291.5 eV was found for the central carbon, and the value of the acetylenic carbon (C3) is only slightly higher by 0.2 eV. For the C1 carbon, the highest value of 292.5 eV was found. The ionization energy value for the formation of a triplet cation is found to be higher than the one of the singlet state for C2, while the reverse is observed for the terminal carbon atoms.

We further investigated the impact of the electronic structure treatment by computing the vertical energies and oscillator strengths of the first two electronic transition using the LR-CCSDT method (and cc-pVDZ basis set) and compared them with corresponding LR-CCSD results. The results are tabulated in Table S7 and illustrated in Figure S3. The separation between the first two electronic excitations, clearly overestimated at CCSD level, is significantly reduced at CCSDT level and close to the experimental value. Moreover, the intensity ratio between the two states changes from 0.58:0.42 to 0.61:0.39.

To conclude this section, we return to the first electronic transitions associated to band A, and discuss the results of our calculations of its vibrational structure. The Wigner samplings shown in Figure S4 indicate a vibrational splitting of the A band. This splitting becomes even more evident in the vibrationally resolved spectra that were obtained from the TI calculations based on the VG and AS potential energy surfaces and that are shown in Figure 5 for CVS-ADC(2)-x. The TD calculations for both fc-CVS-EOM-CCSD and CVS-ADC(2)-x are presented in Figure S5.

Figure 5(a) and (b) show that the first electronic transition has a vibrational splitting

ACCEPTED MANUSCRIPT
The Journal of Chemical Physics
AIP Publishing
This is the author's peer reviewed, accepted manuscript. However, the online version of record will be different from this version once it has been copyedited and typeset.
PLEASE CITE THIS ARTICLE AS DOI: 10.1063/5.0328356

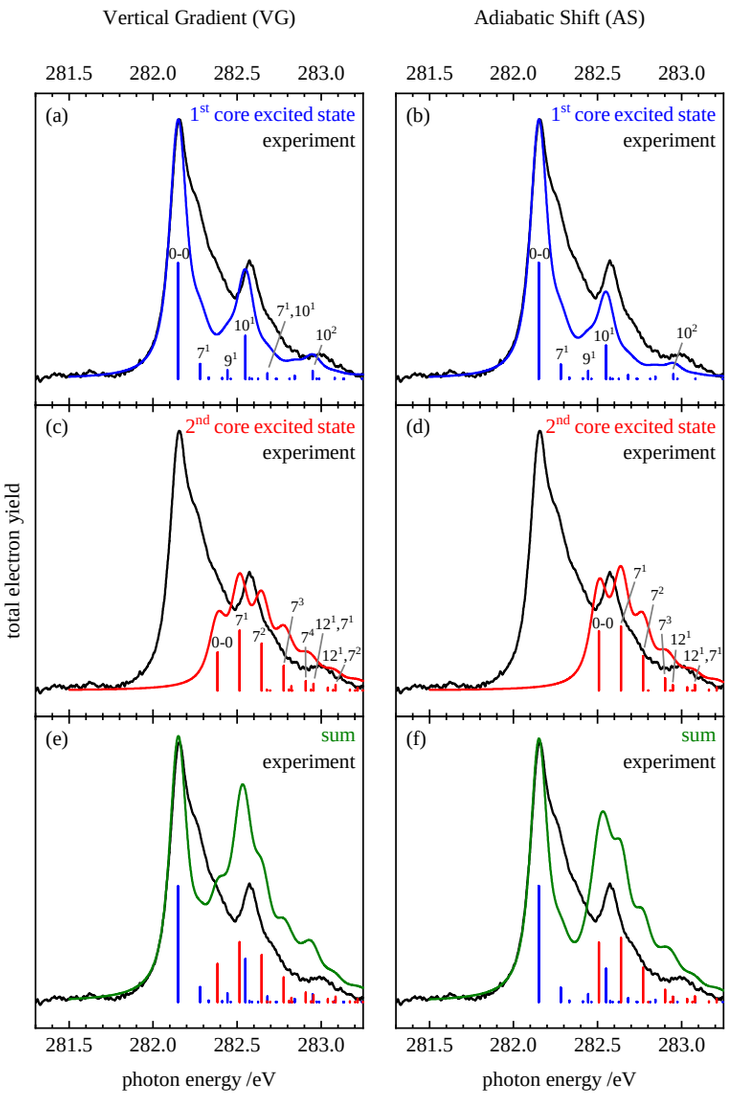


FIG. 5. Comparison between the high-resolution experimental NEXAFS spectrum (black line) and vibrational structure of the (a, b) first, (c, d) second and (e, f) sum of both first and second CVS-ADC(2)-x electronic transitions at 0 K, with PES obtained from the Vertical Gradient (left) and Adiabatic Shift (right) approximations. Vertical lines show the vibronic stick transitions from the vibrational ground state in the initial electronic state obtained using the time-independent formalism.[68] The labels correspond to the vibrational state in the final electronic states, represented as X^v, where X is the normal mode index and v is the number of quanta. All VG results have been shifted by +175 meV and all AS ones by +318 meV to align with the first experimental peak. The spectra have been scaled such that the intensity of the 0-0 band of the first electronic transition overlaps with experiment.

ACCEPTED MANUSCRIPT
The Journal of Chemical Physics
AIP Publishing
This is the author's peer reviewed, accepted manuscript. However, the online version of record will be different from this version once it has been copyedited and typeset.
PLEASE CITE THIS ARTICLE AS DOI: 10.1063/5.0328356

(three bands) consistent with the experimental results. Assignment of which vibronic transitions contribute to each vibrationally resolved band can be done based on the stick transitions from the TI results (with labels X^v, where X indicates the mode involved and v the number of quanta in the mode). The most intense band at 282.16 eV is dominated by the 0-0 transition, with a smaller contribution from the transition from the $v = 0$ level of the electronic ground state to the 7^1 vibrational state of the core excited state. The second band of the progression at 282.58 eV is dominated by the 10^1 vibrational state of the core excited state, with a smaller contribution from 9^1. The third band is mainly 10^2, i.e., a two-quanta vibrational state transition of mode 10. As summarized in Table S8 (and Figure S8), normal mode 10 is the symmetric CH_2 stretching (of C1), mode 7 is dominated by the C1–C2 stretching and mode 9 by the C2–C3 stretching. Inclusion of temperature effects in the TD treatment does not seem to have any visible effect, see Figures S6–S7, which is not surprising giving the level of approximation used for the vibrational calculations.

The vibrationally resolved spectrum of the second electronic transition shown in Figure 5(c) and (d) is an asymmetric band that overlaps with the 10^1 band of the first electronic transition. The band is not peaked at the 0-0 transition, but rather at the 7^1 transition, with its additional quanta $v = 2, 3, 4$, and 5 (together with some excitation of mode 12, which is the C3–H stretch) contributing to the long tail. The sum of the spectra of both the first and second electronic state in Figure 5(e) and (f) indicates that the overall intensity of the band at 282.58 eV is overestimated. As noted earlier, using CCSDT brings the separation between the two electronic states close to the experimental value and also improves their intensity ratio (see Table S7 and Figure S3). While these improvements are *per se* not enough to bring the theoretical and experimental spectra to a quantitative match, they do suggest that the mismatch between theory and experiment is due to the combined effect of approximations in electronic structure used to obtain the input data for the vibronic model, and the choice of vibronic model itself.

By analyzing the spatial distribution of the unpaired electron in microwave measurements, Changala *et al.* recently inferred a 0.61:0.39 ratio between the two nominal resonance structures of propargyl.[10] According to our ADC(2)-x and CCSD calculations, the ratio of the oscillator strengths between the first and second excited states is 0.58:0.42. Using the intensity values obtained from the LR-CCSDT/cc-pVDZ calculations reported in Table S7, we obtain the same ratio of 0.61:0.39 as Changala *et al.*[10] In a simplified one-electron pic-

ACCEPTED MANUSCRIPT
The Journal of Chemical Physics
AIP Publishing
This is the author's peer reviewed, accepted manuscript. However, the online version of record will be different from this version once it has been copyedited and typeset.
PLEASE CITE THIS ARTICLE AS DOI: 10.1063/5.0328356

ture of the electron excitation, this connection between the resonance structures and the lowest core excited states can be qualitatively expected: in the first and second transition the core electron is promoted from C1s orbitals, which differ in the carbon atom localization, to the SOMO. This latter orbital can be considered a weighted linear combination of the two different p-electron systems of the resonant structures shown in Scheme 1, with the p-electron vacancy (unpaired electron spin in the Lewis' structure) located either at C1 (ethynyl methyl resonance structure) or C3 (allenyl resonance structure), respectively. The main contribution to the transition probability will be given by the resonance structure that corresponds to the p-electron system with the core hole/p-electron vacancy space matching. This qualitatively explains the very similar ratios of the calculated oscillator strengths of the first two core electron excitations and the resonance structure weights.

Moreover, the dominant excitation of vibrational mode 10 (symmetric CH_2 stretch of C1) and of mode 7 (C1–C2 stretch) upon transition into the first and second core excited state, respectively, can be related to the change in the molecular geometry upon the C1s excitation. Comparing the structure of the ground state with those of the lowest core excited states (given in Table S9), we note that for the first electronic transition the strongest geometry change is the reduction of the C1–H bond length, and of the C1–C2 bond length upon excitation of the second electronic transition.

From these results, we conclude that the splitting of band A in the experimental spectrum mainly results from the vibrational structure of the first electronic transition (from the ethynyl methyl radical form), specifically the 0-0 transition and the symmetric stretching of the two C1–H bonds, possibly with contributions from the vibrational structure of the second electronic transition (allenyl radical form), due to 0-0 and 7^v transitions ($v = 1 - 5$).

C. Comparison of the propargyl and allyl radical

As both propargyl ($C_3H_3^\bullet$) and allyl ($C_3H_5^\bullet$) are resonance-stabilized hydrocarbon radicals, it is worth to briefly compare their NEXAFS spectra. Both radicals are characterized by a terminal C1s $\rightarrow$ SOMO transition at around 282 eV. The presence of a transition shifted to lower photon energies compared to closed-shell molecules is a characteristic of radicals and has also been observed for the *tert*-butyl radical.[46] In fact, also the shape of band A at 282.2 eV resembles one of the lowest-energy core excitation of the allyl radical, which was

ACCEPTED MANUSCRIPT
The Journal of Chemical Physics
AIP Publishing
This is the author's peer reviewed, accepted manuscript. However, the online version of record will be different from this version once it has been copyedited and typeset.
PLEASE CITE THIS ARTICLE AS DOI: 10.1063/5.0328356

observed at 281.99 eV,[43] and shows a progression that was assigned to a combination of a C–H stretch and an out-of-plane bending mode. However, as the terminal carbon atoms are equivalent in allyl (two equivalent resonance structures), the band is somewhat simpler, as it can be described by a single electronic transition (whereas two electronic transitions contribute to band A of propargyl). In addition, its NEXAFS spectrum shows fewer bands. However, transitions B–E in Figure 2(b) can be related to the central and terminal C1s to LUMO transitions in allyl that were observed at 285.27 eV, 285.71 eV and 287.50 eV.[43]

D. Fragmentation after core excitation

After the resonant core excitation, the core excited states decay via Auger-Meitner processes. The resulting ions were detected by TOF mass spectrometry, and the coincidence setup was used to differentiate between ions from single, double or triple ion events. The fragmentation of the propargyl radical after C1s → SOMO excitation was investigated at 282.2 eV (band A). Figure 6 shows the corresponding mass spectrum for single ion events that was corrected for contributions from off-resonant excitation and unpyrolyzed precursor. The observed fragments and their branching ratios are summarized in Table I.

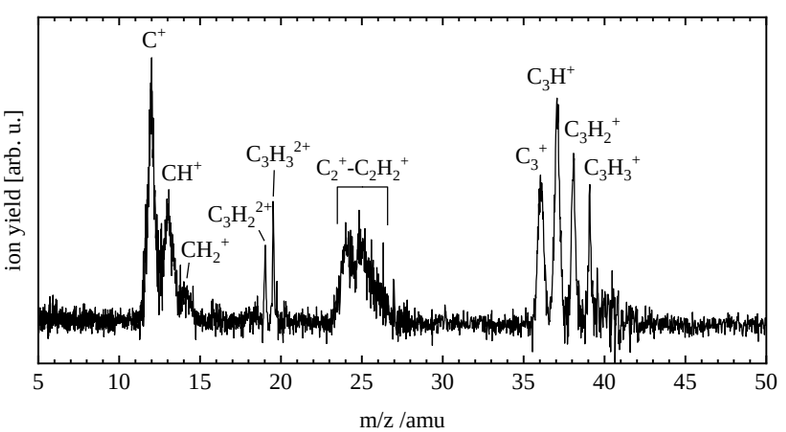


FIG. 6. TOF mass spectrum of single ion events upon excitation of the propargyl radical at band A at 282.2 eV (C1s → SOMO).

The parent ion $C_3H_3^+$ is observed as a sharp signal at m/z 39. Signals at m/z 38, 37 and 36 result from a loss of neutral hydrogens. The signals at m/z 19.5 and 19 belong to the dications $C_3H_3^{2+}$ and $C_3H_2^{2+}$ that are produced by double Auger decay. Most of the fragmentations include the cleavage of one (27%) or both (34%) carbon-carbon bonds. Mass

ACCEPTED MANUSCRIPT
The Journal of Chemical Physics
AIP Publishing
This is the author's peer reviewed, accepted manuscript. However, the online version of record will be different from this version once it has been copyedited and typeset.
PLEASE CITE THIS ARTICLE AS DOI: 10.1063/5.0328356

signals for $C_2H_2^+$ to C_2^+ and CH_2^+ to C^+ are broader because of the kinetic energy released in the fragmentation. From the absence of C_1 or C_2 fragments carrying three hydrogens in the mass spectrum we conclude that no rearrangement of the hydrogen atoms to the higher-energy isomer 1-propenyl cation, $[H_3C–C–C]^+$,[47] takes place in the cationic state. For this isomer the detection of $C_2H_3^+$ or CH_3^+ would have been expected. However, we cannot exclude an isomerization to the lower-energy cyclopropenyl, $C_3H_3^+$, on the cationic surface based on our mass spectrometric data.

We also investigated excitations into higher core excited states at 286.0 eV (band C), 286.6 eV (band D) and 288.1 eV (band E). The corresponding mass spectra and branching ratios can be found in Section S1 in the SI. Compared to the C1s → SOMO transition these excitations show a stronger fragmentation tendency with less C_3 fragments. This is similar to our previous observations for the *tert*-butyl radical and was explained by a preference for spectator decay over participator decay for higher excitation energies.[46]

ACCEPTED MANUSCRIPT
The Journal of Chemical Physics
AIP Publishing
This is the author's peer reviewed, accepted manuscript. However, the online version of record will be different from this version once it has been copyedited and typeset.
PLEASE CITE THIS ARTICLE AS DOI: 10.1063/5.0328356

m/z	species	branching ratio /%
39	$C_3H_3^+$	4
38	$C_3H_2^+$	8
37	C_3H^+	13
36	C_3^+	10
26	$C_2H_2^+$	6
25	C_2H^+	12
24	C_2^+	9
19.5	$C_3H_3^{2+}$	2
19	$C_3H_2^{2+}$	–
14	CH_2^+	4
13	CH^+	13
12	C^+	17
6	C^{2+}	–
others		2

TABLE I. Branching ratios of single ion events after excitation of the propargyl radical at 282.2 eV (band A). Relative intensities were determined from the mass spectrum (Figure 6) by integration. Integrals of overlapping masses were derived from fitting with Gauss functions. The branching ratios were normalized so that all channels sum up to 100%. Very low branching ratios are not specified and are summarized in "others". The error of each branching ratio is estimated to be around ±20% of the respective branching ratio.

ACCEPTED MANUSCRIPT
The Journal of Chemical Physics
AIP Publishing
This is the author's peer reviewed, accepted manuscript. However, the online version of record will be different from this version once it has been copyedited and typeset.
PLEASE CITE THIS ARTICLE AS DOI: 10.1063/5.0328356

IV. CONCLUSION

The NEXAFS spectrum of the propargyl radical at the C1s edge has been recorded using synchrotron radiation. The radical was generated by pyrolysis of propargyl bromide. Although the radical is converted cleanly, conversion of the precursor was not complete and the spectrum of propargyl bromide had to be subtracted. Upon pyrolysis, a new feature emerges at 282.2 eV that is due to C1s → SOMO transitions. By comparison with CVS-ADC(2)-x and fc-CVS-EOM-CCSD computations, it was found that two core excited states ($1\ ^2A_1$ and $2\ ^2A_1$) contribute to this band, the first originating from the excitation of a 1s electron from the terminal C1 atom into a SOMO of ethynyl methyl character, and the second from the excitation of a 1s electron from the terminal C3 atom into a SOMO of allenyl character. Our results are consistent with those of a recent study using hyperfine-resolved microwave spectroscopy and accurate *ab initio* computations,[10] indicating that propargyl possesses a π-delocalized resonance structure of intermediate ethynyl methyl and allenyl character, with non-equal 0.61:0.39 balance between the relative weights of the two resonance structures.

This first band at 282.2 eV exhibits a vibrational progression with a spacing of 420 meV. By means of vertical and adiabatic harmonic calculations, this is mainly assigned to the symmetric CH_2 stretching mode of the first core excited state (C1 1s → SOMO of ethynyl methyl), possibly with contributions from the vibrational structure of the second core excited state (C3 1s → SOMO of allenyl). In addition, several bands at higher photon energy can be assigned to transitions from C2 and C3 into the π^* orbitals. Overall, the appearance of the spectrum resembles the one of the allyl radical, $C_3H_5^{\bullet}$.

Core ionization energies between 291.5 eV and 292.6 eV for ionization into the singlet cation were computed for the different carbon atoms. Compared to the singlet cation, the ionization energy to the triplet cation is lower for the two terminal C atoms, but is slightly higher for the central one.

The fragmentation pattern upon (terminal) C1s → SOMO excitation shows peaks of the molecular parent cation and dication, but also a broad distribution of fragments including loss of one to three H-atoms, and cleavage of one or both C–C bonds. Interestingly, no CH_3^+ is observed, indicating the absence of an isomerization to the 1-propenyl cation. In comparison, excitation to higher core excited states is associated with a more pronounced

ACCEPTED MANUSCRIPT
The Journal of Chemical Physics
AIP Publishing
This is the author's peer reviewed, accepted manuscript. However, the online version of record will be different from this version once it has been copyedited and typeset.
PLEASE CITE THIS ARTICLE AS DOI: 10.1063/5.0328356

fragmentation dominated by the almost complete disappearance of the molecular cation and an increasing dominance of C_1^+ fragment ions.

V. SUPPLEMENTARY MATERIAL

See supplementary information for mass spectra at higher photon energies, additional computational details and results.

VI. ACKNOWLEDGMENTS

The work has been financially supported by the German Science Foundation (DFG), contract FI 575/13-2. D.S. acknowledges a fellowship by the Fonds der Chemischen Industrie (FCI). We acknowledge invaluable discussions with Dr. Fabrizio Santoro and Dr. Iulia Emilia Brumboiu. J.P. acknowledges financial support from the Technical University of Denmark within the Ph.D. Alliance Programme. S.C. thanks Hamburg's Cluster of Excellence "CUI: Advanced Imaging of Matter" for the 2024 Mildred Dresselhaus Prize. S.C. and T.J.v.B. acknowledge funding from the Novo Nordisk Foundation (NNF Grant No. NNFSA220080996). S.S. and A.B. acknowledge financial support from the University of Rome "La Sapienza", project Ateneo 2024 RG1241909C0A0A47, and a PhD fellowship, respectively.

DATA AVAILABILITY STATEMENT

The data are available from the authors upon reasonable request.

VII. AUTHOR CONTRIBUTIONS

D.S., A.R., E.K., V.v.L., A.B., M.A., S.S., and I.F. designed and conducted the experiments. T.J.v.B., J.P. and S.C. designed the computational protocols, carried out the calculations and characterized the NEXAFS spectra based on the *ab initio* results. D.S. analyzed the experimental data and wrote the first draft of the paper; T.J.v.B. and S.C. wrote the parts concerning the computational results. All authors discussed the interpretation of the results and contributed to the final version of the paper.

ACCEPTED MANUSCRIPT
The Journal of Chemical Physics
AIP Publishing
This is the author's peer reviewed, accepted manuscript. However, the online version of record will be different from this version once it has been copyedited and typeset.
PLEASE CITE THIS ARTICLE AS DOI: 10.1063/5.0328356

REFERENCES

[1]H. Richter and J. Howard, "Formation of polycyclic aromatic hydrocarbons and their growth to soot—a review of chemical reaction pathways," Prog. Energy Combust. Sci. **26**, 565–608 (2000).

[2]M. E. Kress, A. G. Tielens, and M. Frenklach, "The 'soot line': Destruction of presolar polycyclic aromatic hydrocarbons in the terrestrial planet-forming region of disks," Adv. Space Res. **46**, 44–49 (2010).

[3]Z. D. Levey, B. A. Laws, S. P. Sundar, K. Nauta, S. H. Kable, G. da Silva, J. F. Stanton, and T. W. Schmidt, "PAH Growth in Flames and Space: Formation of the Phenalenyl Radical," J. Phys. Chem. A **126**, 101–108 (2022).

[4]A. N. Byrne, C. Xue, I. R. Cooke, M. C. McCarthy, and B. A. McGuire, "Astrochemical modeling of propargyl radical chemistry in TMC-1," ApJ **957**, 88 (2023).

[5]A. G. G. M. Tielens, "The molecular universe," Rev. Mod. Phys. **85**, 1021–1081 (2013).

[6]A. G. G. M. Tielens, "Interstellar polycyclic aromatic hydrocarbon molecules," Annu. Rev. Astron. Astrophys. **46**, 289–337 (2008).

[7]U. Alkemade and K.-H. Homann, "Formation of C_6H_6 Isomers by Recombination of Propynyl in the System Sodium Vapour/Propynylhalide," Z. Phys. Chem., Neue Folge **161**, 19–34 (1989).

[8]S. E. Stein, J. A. Walker, M. M. Suryan, and A. Fahr, "A new path to benzene in flames," Symp. (Int.) Combust. **23**, 85–90 (1991).

[9]P. Botschwina and R. Oswald, "Calculated photoelectron spectra of isotopomers of the propargyl radical (H_2C_3H): An explicitly correlated coupled cluster study," Chem. Phys. **378**, 4–10 (2010).

[10]P. B. Changala, P. R. Franke, J. F. Stanton, G. B. Ellison, and M. C. McCarthy, "Direct Probes of π-Delocalization in Prototypical Resonance-Stabilized Radicals: Hyperfine-Resolved Microwave Spectroscopy of Isotopic Propargyl and Cyanomethyl," J. Am. Chem. Soc. **146**, 1512–1521 (2024).

[11]Agúndez, M., Cabezas, C., Tercero, B., Marcelino, N., Gallego, J. D., de Vicente, P., and Cernicharo, J., "Discovery of the propargyl radical (CH_2CCH) in TMC-1: One of the most abundant radicals ever found and a key species for cyclization to benzene in cold dark clouds," Astron. Astrophys. **647**, L10 (2021).

ACCEPTED MANUSCRIPT
The Journal of Chemical Physics
AIP Publishing
This is the author's peer reviewed, accepted manuscript. However, the online version of record will be different from this version once it has been copyedited and typeset.
PLEASE CITE THIS ARTICLE AS DOI: 10.1063/5.0328356

[12]Agúndez, M., Marcelino, N., Cabezas, C., Fuentetaja, R., Tercero, B., de Vicente, P., and Cernicharo, J., "Detection of the propargyl radical at λ 3 mm," Astron. Astrophys. **657**, A96 (2022).

[13]W. G. D. P. Silva, J. Cernicharo, S. Schlemmer, N. Marcelino, J.-C. Loison, M. Agúndez, D. Gupta, V. Wakelam, S. Thorwirth, C. Cabezas, B. Tercero, J. L. Doménech, R. Fuentetaja, W.-J. Kim, P. de Vicente, and O. Asvany, "Discovery of H_2CCCH^+ in TMC-1," Astron. Astrophys. **676**, L1 (2023).

[14]K. Tanaka, Y. Sumiyoshi, Y. Ohshima, Y. Endo, and K. Kawaguchi, "Pulsed discharge nozzle Fourier transform microwave spectroscopy of the propargyl radical (H_2CCCH)," J. Chem. Phys. **107**, 2728–2733 (1997).

[15]E. Hebrard, M. Dobrijevic, J. C. Loison, A. Bergeat, K. M. Hickson, and F. Caralp, "Photochemistry of C_3H_p hydrocarbons in Titan's stratosphere revisited," Astron. Astrophys. **552**, A132 (2013).

[16]E. Herbst and C. M. Leung, "Gas-phase production of complex hydrocarbons, cyanopolyynes, and related compounds in dense interstellar clouds," Astrophys. J. Suppl. Ser. **69**, 271–300 (1989).

[17]M. E. Jacox and D. E. Milligan, "Matrix isolation study of the vacuum ultraviolet photolysis of allene and methylacetylene. vibrational and electronic spectra of the species C_3, C_3H, C_3H_2, and C_3H_3," Chem. Phys. **4**, 45–61 (1974).

[18]E. B. Jochnowitz, X. Zhang, M. R. Nimlos, M. E. Varner, J. F. Stanton, and G. B. Ellison, "Propargyl radical: ab initio anharmonic modes and the polarized infrared absorption spectra of matrix-isolated $HCCCH_2$," J. Phys. Chem. A **109**, 3812–21 (2005).

[19]D. A. Ramsay and P. Thistlethwaite, "The electronic absorption spectrum of the propargyl radical," Can. J. Phys. **44**, 1381–1386 (1966).

[20]A. Fahr and A. H. Laufer, "UV-absorption spectra of the radical transients generated from the 193-nm photolysis of allene, propyne, and 2-butyne," J. Phys. Chem. A **109**, 2534–9 (2005).

[21]P. Hemberger, M. Lang, B. Noller, I. Fischer, C. Alcaraz, B. K. Cunha de Miranda, G. A. Garcia, and H. Soldi-Lose, "Photoionization of Propargyl and Bromopropargyl Radicals: A Threshold Photoelectron Spectroscopic Study," J. Phys. Chem. A **115**, 2225–2230 (2011).

[22]U. Jacovella, B. Gans, and F. Merkt, "On the adiabatic ionization energy of the propargyl radical," J. Chem. Phys. **139**, 084308 (2013).

ACCEPTED MANUSCRIPT
The Journal of Chemical Physics
AIP Publishing
This is the author's peer reviewed, accepted manuscript. However, the online version of record will be different from this version once it has been copyedited and typeset.
PLEASE CITE THIS ARTICLE AS DOI: 10.1063/5.0328356

[23]G. A. Garcia, B. Gans, J. Krüger, F. Holzmeier, A. Röder, A. Lopes, C. Fittschen, C. Alcaraz, and J.-C. Loison, "Valence shell threshold photoelectron spectroscopy of C_3H_x (x = 0-3)," Phys. Chem. Chem. Phys. **20**, 8707–8718 (2018).

[24]J. D. Savee, B. Sztáray, P. Hemberger, J. Zádor, A. Bodi, and D. L. Osborn, "Unimolecular isomerisation of 1,5-hexadiyne observed by threshold photoelectron photoion coincidence spectroscopy," Faraday Discuss. **238**, 645–664 (2022).

[25]H.-J. Deyerl, I. Fischer, and P. Chen, "Photodissociation dynamics of the propargyl radical," J. Chem. Phys. **111**, 3441–3448 (1999).

[26]X. Zheng, Y. Song, and J. Zhang, "Ultraviolet photodissociation dynamics of the propargyl radical," J. Phys. Chem. A **113**, 4604–12 (2009).

[27]B. M. Broderick, N. Suas-David, N. Dias, and A. G. Suits, "Isomer-specific detection in the uv photodissociation of the propargyl radical by chirped-pulse mm-wave spectroscopy in a pulsed quasi-uniform flow," Phys. Chem. Chem. Phys. **20**, 5517–5529 (2018).

[28]I. Savić and D. Gerlich, "Temperature variable ion trap studies of $C_3H_n^+$ with H_2 and HD," Phys. Chem. Chem. Phys. **7**, 1026–1035 (2005).

[29]I. Savić, S. Schlemmer, and D. Gerlich, "Low-Temperature Experiments on the Formation of Deuterated $C_3H_3^+$," ApJ **621**, 1163 (2005).

[30]L. Zhao, W. Lu, M. Ahmed, M. V. Zagidullin, V. N. Azyazov, A. N. Morozov, A. M. Mebel, and R. I. Kaiser, "Gas-phase synthesis of benzene via the propargyl radical self-reaction," Sci. Adv. **7**, eabf0360 (2021).

[31]H. R. Hrodmarsson, G. A. Garcia, L. Bourehil, L. Nahon, B. Gans, S. Boyé-Péronne, J.-C. Guillemin, and J.-C. Loison, "The isomer distribution of C_6H_6 products from the propargyl radical gas-phase recombination investigated by threshold-photoelectron spectroscopy," Commun. Chem. **7**, 156 (2024).

[32]P. Constantinidis, F. Hirsch, I. Fischer, A. Dey, and A. M. Rijs, "Products of the Propargyl Self-Reaction at High Temperatures Investigated by IR/UV Ion Dip Spectroscopy," J. Phys. Chem. A **121**, 181–191 (2017).

[33]J. A. Miller and S. J. Klippenstein, "The Recombination of Propargyl Radicals and Other Reactions on a C_6H_6 Potential," J. Phys. Chem. A **107**, 7783–7799 (2003).

[34]J. D. Savee, T. M. Selby, O. Welz, C. A. Taatjes, and D. L. Osborn, "Time- and isomer-resolved measurements of sequential addition of acetylene to the propargyl radical," J. Phys. Chem. Lett. **6**, 4153–8 (2015).

ACCEPTED MANUSCRIPT
The Journal of Chemical Physics
AIP Publishing
This is the author's peer reviewed, accepted manuscript. However, the online version of record will be different from this version once it has been copyedited and typeset.
PLEASE CITE THIS ARTICLE AS DOI: 10.1063/5.0328356

[35]T. M. Selby, F. Goulay, S. Soorkia, A. Ray, A. W. Jasper, S. J. Klippenstein, A. N. Morozov, A. M. Mebel, J. D. Savee, C. A. Taatjes, and D. L. Osborn, "Radical-Radical Reactions in Molecular Weight Growth: The Phenyl + Propargyl Reaction," J. Phys. Chem. A **127**, 2577–2590 (2023).

[36]Z. Yang, G. R. Galimova, C. He, S. J. Goettl, D. Paul, W. Lu, M. Ahmed, A. M. Mebel, X. Li, and R. I. Kaiser, "Gas-phase formation of the resonantly stabilized 1-indenyl ($C_9H_7^{\bullet}$) radical in the interstellar medium," Sci. Adv. **9**, eadi5060 (2023).

[37]J. Zhang, J. Gao, H. Wang, J. Guan, G. Xu, L. Xing, D. G. Truhlar, and Z. Wang, "Less-dominant resonance configuration of propargyl radical leads to a growth mechanism for polycyclic aromatic hydrocarbons that preserves the cyclopenta ring," J. Am. Chem. Soc. **147**, 9283–9293 (2025).

[38]P. Lindstedt, L. Maurice, and M. Meyer, "Thermodynamic and kinetic issues in the formation and oxidation of aromatic species," Faraday Discuss. **119**, 409–432 (2002).

[39]A. Matsugi and A. Miyoshi, "Computational study on the recombination reaction between benzyl and propargyl radicals," Int. J. Chem. Kinet. **44**, 206–218 (2012).

[40]A. N. Morozov and A. M. Mebel, "Theoretical study of the reaction mechanism and kinetics of the phenyl + propargyl association," Phys. Chem. Chem. Phys. **22**, 6868–6880 (2020).

[41]R. Arns, R. McClish, P. Hemberger, A. Bodi, J. Bouwman, T. Kasper, and D. Schleier, "Is Phenylnitrene a Missing Link in the Formation of Polycyclic Aromatic Nitrogen Heterocycles?" Angew. Chem. Int. Ed. **64**, e202503940 (2025).

[42]P. Stäuber, S. Doty, E. Van Dishoeck, and A. Benz, "X-ray chemistry in the envelopes around young stellar objects," Astron. Astrophys. **440**, 949–966 (2005).

[43]M. Alagia, E. Bodo, P. Decleva, S. Falcinelli, A. Ponzi, R. Richter, and S. Stranges, "The soft X-ray absorption spectrum of the allyl free radical," Phys. Chem. Chem. Phys. **15**, 1310–1318 (2013).

[44]M. Alagia, M. Lavollée, R. Richter, U. Ekström, V. Carravetta, D. Stranges, B. Brunetti, and S. Stranges, "Probing the potential energy surface by high-resolution x-ray absorption spectroscopy: The umbrella motion of the core-excited CH_3 free radical," Phys. Rev. A **76**, 022509 (2007).

[45]U. Ekström, V. Carravetta, M. Alagia, M. Lavollée, R. Richter, C. Bolcato, and S. Stranges, "The umbrella motion of core-excited CH_3 and CD_3 methyl radicals," J. Chem. Phys. **128**, 044302 (2008).

ACCEPTED MANUSCRIPT
The Journal of Chemical Physics
AIP Publishing
This is the author's peer reviewed, accepted manuscript. However, the online version of record will be different from this version once it has been copyedited and typeset.
PLEASE CITE THIS ARTICLE AS DOI: 10.1063/5.0328356

[46]D. Schaffner, T. Juncker von Buchwald, E. Karaev, M. Alagia, R. Richter, S. Stranges, S. Coriani, and I. Fischer, "The x-ray absorption spectrum of the tert-butyl radical: An experimental and computational investigation," J. Chem. Phys. **161**, 034309 (2024).

[47]S. Reinwardt, P. Cieslik, T. Buhr, A. Perry-Sassmannshausen, S. Schippers, A. Müller, F. Trinter, and M. Martins, "Isomer-specific photofragmentation of $C_3H_3^+$ at the carbon K-edge," Phys. Chem. Chem. Phys. **26**, 15519–15529 (2024).

[48]R. R. Blyth, R. Delaunay, M. Zitnik, J. Krempasky, R. Krempaska, J. Slezak, K. C. Prince, R. Richter, M. Vondracek, R. Camilloni, L. Avaldi, M. Coreno, G. Stefani, C. Furlani, M. de Simone, S. Stranges, and M. Y. Adam, "The high resolution Gas Phase Photoemission beamline, Elettra," J. Electron Spectrosc. Relat. Phenom. **101-103**, 959–964 (1999).

[49]M. Alagia, L. Avaldi, M. Coreno, R. Camilloni, C. Furlani, K. C. Prince, R. Richter, M. de Simone, G. Stefani, and S. Stranges, "The gas phase photoemission beamline at Elettra," Synchrotron Radiat. News **16**, 19–27 (2003).

[50]M. de Simone, M. Coreno, M. Alagia, R. Richter, and K. C. Prince, "Inner shell excitation spectroscopy of the tetrahedral molecules CX_4 (X = H, F, Cl)," J. Phys. B: At. Mol. Opt. Phys. **35**, 61 (2002).

[51]M. L. Vidal, X. Feng, E. Epifanovsky, A. I. Krylov, and S. Coriani, "A New and Efficient Equation-of-Motion Coupled-Cluster Framework for Core-Excited and Core-Ionized States," J. Chem. Theory Comput. **15**, 3117–3133 (2019).

[52]A. Dreuw and M. Wormit, "The algebraic diagrammatic construction scheme for the polarization propagator for the calculation of excited states," WIREs Comput. Mol. Sci. **5**, 82–95 (2015).

[53]E. Epifanovsky, A. T. B. Gilbert, X. Feng, J. Lee, Y. Mao, N. Mardirossian, P. Pokhilko, A. F. White, M. P. Coons, A. L. Dempwolff, Z. Gan, D. Hait, P. R. Horn, L. D. Jacobson, I. Kaliman, J. Kussmann, A. W. Lange, K. U. Lao, D. S. Levine, J. Liu, S. C. McKenzie, A. F. Morrison, K. D. Nanda, F. Plasser, D. R. Rehn, M. L. Vidal, Z.-Q. You, Y. Zhu, B. Alam, B. J. Albrecht, A. Aldossary, E. Alguire, J. H. Andersen, V. Athavale, D. Barton, K. Begam, A. Behn, N. Bellonzi, Y. A. Bernard, E. J. Berquist, H. G. A. Burton, A. Carreras, K. Carter-Fenk, R. Chakraborty, A. D. Chien, K. D. Closser, V. Cofer-Shabica, S. Dasgupta, M. de Wergifosse, J. Deng, M. Diedenhofen, H. Do, S. Ehlert, P.-T. Fang, S. Fatehi, Q. Feng, T. Friedhoff, J. Gayvert, Q. Ge, G. Gidofalvi, M. Goldey, J. Gomes, C. E. González-Espinoza, S. Gulania, A. O. Gunina, M. W. D. Hanson-Heine, P. H. P.

ACCEPTED MANUSCRIPT
The Journal of Chemical Physics
AIP Publishing
This is the author's peer reviewed, accepted manuscript. However, the online version of record will be different from this version once it has been copyedited and typeset.
PLEASE CITE THIS ARTICLE AS DOI: 10.1063/5.0328356

Harbach, A. Hauser, M. F. Herbst, M. Hernández Vera, M. Hodecker, Z. C. Holden, S. Houck, X. Huang, K. Hui, B. C. Huynh, M. Ivanov, A. Jász, H. Ji, H. Jiang, B. Kaduk, S. Kähler, K. Khistyaev, J. Kim, G. Kis, P. Klunzinger, Z. Koczor-Benda, J. H. Koh, D. Kosenkov, L. Koulias, T. Kowalczyk, C. M. Krauter, K. Kue, A. Kunitsa, T. Kus, I. Ladjánszki, A. Landau, K. V. Lawler, D. Lefrancois, S. Lehtola, R. R. Li, Y.-P. Li, J. Liang, M. Liebenthal, H.-H. Lin, Y.-S. Lin, F. Liu, K.-Y. Liu, M. Loipersberger, A. Luenser, A. Manjanath, P. Manohar, E. Mansoor, S. F. Manzer, S.-P. Mao, A. V. Marenich, T. Markovich, S. Mason, S. A. Maurer, P. F. McLaughlin, M. F. S. J. Menger, J.-M. Mewes, S. A. Mewes, P. Morgante, J. W. Mullinax, K. J. Oosterbaan, G. Paran, A. C. Paul, S. K. Paul, F. Pavošević, Z. Pei, S. Prager, E. I. Proynov, Á. Rák, E. Ramos-Cordoba, B. Rana, A. E. Rask, A. Rettig, R. M. Richard, F. Rob, E. Rossomme, T. Scheele, M. Scheurer, M. Schneider, N. Sergueev, S. M. Sharada, W. Skomorowski, D. W. Small, C. J. Stein, Y.-C. Su, E. J. Sundstrom, Z. Tao, J. Thirman, G. J. Tornai, T. Tsuchimochi, N. M. Tubman, S. P. Veccham, O. Vydrov, J. Wenzel, J. Witte, A. Yamada, K. Yao, S. Yeganeh, S. R. Yost, A. Zech, I. Y. Zhang, X. Zhang, Y. Zhang, D. Zuev, A. Aspuru-Guzik, A. T. Bell, N. A. Besley, K. B. Bravaya, B. R. Brooks, D. Casanova, J.-D. Chai, S. Coriani, C. J. Cramer, G. Cserey, A. E. DePrince, R. A. DiStasio, A. Dreuw, B. D. Dunietz, T. R. Furlani, W. A. Goddard, S. Hammes-Schiffer, T. Head-Gordon, W. J. Hehre, C.-P. Hsu, T.-C. Jagau, Y. Jung, A. Klamt, J. Kong, D. S. Lambrecht, W. Liang, N. J. Mayhall, C. W. McCurdy, J. B. Neaton, C. Ochsenfeld, J. A. Parkhill, R. Peverati, V. A. Rassolov, Y. Shao, L. V. Slipchenko, T. Stauch, R. P. Steele, J. E. Subotnik, A. J. W. Thom, A. Tkatchenko, D. G. Truhlar, T. Van Voorhis, T. A. Wesolowski, K. B. Whaley, H. L. Woodcock, P. M. Zimmerman, S. Faraji, P. M. W. Gill, M. Head-Gordon, J. M. Herbert, and A. I. Krylov, "Software for the frontiers of quantum chemistry: An overview of developments in the Q-Chem 5 package," J. Chem. Phys. **155**, 084801 (2021).

[54]T. Clark, J. Chandrasekhar, G. W. Spitznagel, and P. V. R. Schleyer, "Efficient diffuse function-augmented basis sets for anion calculations. III. The 3-21+G basis set for first-row elements, Li-F," J. Comput. Chem. **4**, 294–301 (1983).

[55]R. Krishnan, J. S. Binkley, R. Seeger, and J. A. Pople, "Self-consistent molecular orbital methods. XX. A basis set for correlated wave functions," J. Chem. Phys. **72**, 650–654 (1980).

ACCEPTED MANUSCRIPT
The Journal of Chemical Physics
AIP Publishing
This is the author's peer reviewed, accepted manuscript. However, the online version of record will be different from this version once it has been copyedited and typeset.
PLEASE CITE THIS ARTICLE AS DOI: 10.1063/5.0328356

[56]O. Marchetti and H.-J. Werner, "Accurate calculations of intermolecular interaction energies using explicitly correlated wave functions," Phys. Chem. Chem. Phys. **10**, 3400–3409 (2008).

[57]T. H. Dunning, "Gaussian basis sets for use in correlated molecular calculations. I. The atoms boron through neon and hydrogen," J. Chem. Phys. **90**, 1007–1023 (1989).

[58]R. A. Kendall, T. H. Dunning, and R. J. Harrison, "Electron affinities of the first-row atoms revisited. systematic basis sets and wave functions," J. Chem. Phys. **96**, 6796–6806 (1992).

[59]S. Coriani and H. Koch, "Communication: X-ray absorption spectra and core-ionization potentials within a core-valence separated coupled cluster framework," J. Chem. Phys. **143**, 181103 (2015).

[60]M. Kállay, P. R. Nagy, D. Mester, Z. Rolik, G. Samu, J. Csontos, J. Csóka, P. B. Szabó, L. Gyevi-Nagy, B. Hégely, I. Ladjánszki, L. Szegedy, B. Ladóczki, K. Petrov, M. Farkas, P. D. Mezei, and Á. Ganyecz, "The mrcc program system: Accurate quantum chemistry from water to proteins," J. Chem. Phys. **152**, 074107 (2020).

[61]T. B. Adler, G. Knizia, and H.-J. Werner, "A simple and efficient CCSD(T)-F12 approximation," J. Chem. Phys. **127**, 221106 (2007).

[62]G. Knizia, T. B. Adler, and H.-J. Werner, "Simplified CCSD(T)-F12 methods: Theory and benchmarks," J. Chem. Phys. **130**, 054104 (2009).

[63]K. A. Peterson, T. B. Adler, and H.-J. Werner, "Systematically convergent basis sets for explicitly correlated wavefunctions: The atoms H, He, B-Ne, and Al-Ar," J. Chem. Phys. **128**, 084102 (2008).

[64]A. I. Krylov, "From orbitals to observables and back," J. Chem. Phys. **153**, 080901 (2020).

[65]DTU Computing Center, "DTU Computing Center resources," (2024), https://doi.org/10.48714/DTU.HPC.0001.

[66]R. Crespo-Otero and M. Barbatti, "Spectrum simulation and decomposition with nuclear ensemble: formal derivation and application to benzene, furan and 2-phenylfuran," Theor. Chem. Acc. **131**, 1237 (2012).

[67]P. J. Stephens, F. J. Devlin, C. F. Chabalowski, and M. J. Frisch, "Ab initio calculation of vibrational absorption and circular dichroism spectra using density functional force fields," J. Phys. Chem. **98**, 11623–11627 (1994).

ACCEPTED MANUSCRIPT
The Journal of Chemical Physics
AIP Publishing
This is the author's peer reviewed, accepted manuscript. However, the online version of record will be different from this version once it has been copyedited and typeset.
PLEASE CITE THIS ARTICLE AS DOI: 10.1063/5.0328356

[68]F. J. Avila Ferrer and F. Santoro, "Comparison of vertical and adiabatic harmonic approaches for the calculation of the vibrational structure of electronic spectra," Phys. Chem. Chem. Phys. **14**, 13549–13563 (2012).

[69]J. Cerezo and F. Santoro, "*FCclasses3*: Vibrationally-resolved spectra simulated at the edge of the harmonic approximation," J. Comput. Chem. **44**, 626–643 (2023).

[70]P. Macak, Y. Luo, and H. Ågren, "Simulations of vibronic profiles in two-photon absorption," Chem. Phys. Lett. **330**, 447–456 (2000).

[71]M. Biczysko, J. Bloino, F. Santoro, and V. Barone, "Time-independent approaches to simulate electronic spectra lineshapes: From small molecules to macrosystems," in *Computational strategies for spectroscopy* (Wiley Online Library, 2012) pp. 361–443.

[72]M. Frisch, G. W. Trucks, H. B. Schlegel, G. E. Scuseria, M. Robb, J. R. Cheeseman, G. Scalmani, V. Barone, G. A. Petersson, H. Nakatsuji, *et al.*, "Gaussian 16," (2016).

[73]Q. Sun, T. C. Berkelbach, N. S. Blunt, G. H. Booth, S. Guo, Z. Li, J. Liu, J. D. McClain, E. R. Sayfutyarova, S. Sharma, S. Wouters, and G. K.-L. Chan, "`PySCF`: the Python-based simulations of chemistry framework," WIRES Comput. Mol. Sci. **8**, e1340 (2018).

[74]Q. Sun, X. Zhang, S. Banerjee, P. Bao, M. Barbry, N. S. Blunt, N. A. Bogdanov, G. H. Booth, J. Chen, Z.-H. Cui, J. J. Eriksen, Y. Gao, S. Guo, J. Hermann, M. R. Hermes, K. Koh, P. Koval, S. Lehtola, Z. Li, J. Liu, N. Mardirossian, J. D. McClain, M. Motta, B. Mussard, H. Q. Pham, A. Pulkin, W. Purwanto, P. J. Robinson, E. Ronca, E. R. Sayfutyarova, M. Scheurer, H. F. Schurkus, J. E. T. Smith, C. Sun, S.-N. Sun, S. Upadhyay, L. K. Wagner, X. Wang, A. White, J. D. Whitfield, M. J. Williamson, S. Wouters, J. Yang, J. M. Yu, T. Zhu, T. C. Berkelbach, S. Sharma, A. Y. Sokolov, and G. K.-L. Chan, "Recent developments in the `PySCF` program package," J. Chem. Phys. **153**, 024109 (2020).

[75]M. F. Herbst, M. Scheurer, T. Fransson, D. R. Rehn, and A. Dreuw, "`adcc`: A versatile toolkit for rapid development of algebraic-diagrammatic construction methods," WIREs Comput. Mol. Sci. **10**, e1462 (2020).

[76]I. E. Brumboiu, "`cvs-adc-grad`," `https://gitlab.com/iubr/cvs-adc-grad` (2025).

[77]L.-P. Wang and C. Song, "Geometry optimization made simple with translation and rotation coordinates," J. Chem. Phys. **144**, 214108 (2016).

[78]J. L. Holmes and F. P. Lossing, "The reactivity of $[C_3H_3^+]$ ions; a thermochemical study," Can. J. Chem. **57**, 249–252 (1979).

[79]T. Schüßler, W. Roth, T. Gerber, C. Alcaraz, and I. Fischer, "The VUV photochemistry of radicals: C_3H_3 and C_2H_5," Phys. Chem. Chem. Phys. **7**, 819–825 (2005).

AIP Publishing
The Journal of Chemical Physics
ACCEPTED MANUSCRIPT
This is the author's peer reviewed, accepted manuscript. However, the online version of record will be different from this version once it has been copyedited and typeset.
PLEASE CITE THIS ARTICLE AS DOI: 10.1063/5.0328356